

G.L. PANKANIN, J. BERLIŃSKI, R. CHMIELEWSKI

Warsaw University of Technology  
Institute of Electronic Systems  
Poland, e-mail: g.pankanin@ise.pw.edu.pl

## ANALYTICAL MODELLING OF KARMAN VORTEX STREET

A new approach to the Karman vortex street modelling is presented. The model is based on observations of the Karman vortex street. The idea of the model is based on fundamental mechanical formulas. According to the model, vortices are created on the bluff body surface in the area of the boundary separation. The grow-up of the vortex results from the process looking like a reeling of some amount of the liquid on the vortex core during its rolling downstream on the surface of unmoved stagnation region. This process is represented in the model as a succeeding addition layer attachment. The vortex evolution has been divided into three stages. Hence three zones downstream the bluff body are distinguished: intensive development, stabilization and vortices decay. Influence of the fluid viscosity on the development process and rotation energy of the vortex has been also analyzed.

Keywords: numerical modelling, Karman vortex street, vortex meter

### 1. INTRODUCTION

Numerous articles are devoted to the vortex shedding phenomena being the basis of the vortex meter. In spite of the fact that the vortex meter has been manufactured since early 70's of XX<sup>th</sup> century, the phenomenon is not yet fully recognized. It should be underlined that only comprehensive knowledge of applied phenomena can ensure successful manufacturing. This sentence concerns, however, not only the vortex meter, but all devices produced for the measurement of physical quantities. In the case of the vortex meter, the process of recognition has been very complicated and carried out with application of various research methods. In early works, the "try and error technique" has been used [1-4]. In spite of the simplicity of the method, important works carried out by Cousins et al. [1] led to general recommendations concerning optimal bluff body to pipe diameter ratio for some shapes of the vortex generator. Also the recommendations concerning the existence of sharp edges in the bluff body (generator of vortices) have appeared as the main result of the investigations.

Introduction of quality parameters [5-8] enabled more efficient bluff body optimization. Later works [9] proved also the possibility of optimization of the sensor location. Flow visualization played a very important role in Karman vortex street investigations, it has been used from the very beginning - already by Leonardo da Vinci in the XVI<sup>th</sup> century. Later numerous researchers applied flow visualization for the observation of phenomena appearing in the vortex meter [4, 10-16]. It should be noted that nearly all considerable achievements in vortex meter design have been supported by flow visualization investigations. Introduction of the slit into the circular cylinder by Igarashi [10,11,13] and the new shape of the rear part of the bluff body proposed by Popiel et al. [12] can be mentioned as such examples. Image processing application created new possibilities in the flow visualization picture analysis. Quantitative information concerning the Karman vortex street has been obtained. In the course of the investigations carried out by

Pankanin [17], the distance between consecutive vortices as well as convection velocity have been determined.

The hot-wire anemometer for velocity flow field determination also has been used as a tool for the phenomena investigations [18-21]. The velocity and turbulence distributions in the whole plane downstream the bluff body have been used for better understanding of the phenomena. Determination of certain parameters of the Karman vortex street also has been stated [19].

A new approach to the problem of phenomenon investigations is proposed in the article. A phenomenological model based on fundamental mechanical equations has been created. At first glance it can be perceived as too much simplified or even naive. Results of simulation, however, are amazingly consistent with the ones attained with application of other methods.

## 2. VORTEX METHOD OF FLOW MEASUREMENT



Fig.1. Karman vortex street.

The vortex flow meter is based on vortex shedding on the obstacle placed in the flowing fluid (Fig.1.). The frequency of vortices shedding alternatively on both sides of the bluff body is a linear function of the flow velocity:

$$f = S_T \frac{v}{d}. \quad (1)$$

The Strouhal number is constant in a very wide range of flow velocities and independent of the physical properties of the medium. Hence the feasibility of the flow meter design of high rangeability (even 100:1). The Eq. (1) is fulfilled for liquids and as well for gases. The mechanism of vortex shedding is very complex. It was the subject of consideration of various researchers. The most significant were the works carried out by Birkhoff [22] and Gerrard [23]. Although their models do not fully explain the phenomena, they can be the basis for understanding vortex shedding.

From the point of view of the vortex shedding application for flow measurement, the regularity and strength of generated vortices are the most important phenomena features. It is well-known from the early investigations [1] that the quality of generated vortices mainly depends on the shape and dimensions of the bluff body (strictly speaking - on the ratio of the bluff body characteristic dimension to the pipe diameter). Hence the bluff body as the measuring signal origin should be optimized primarily. It is worth to underline that although the vortex meter is linear, the value of its nonlinearity error depends on the bluff body geometry. Especially

important is the stabilization of the separation point, reached due to sharp edges on the bluff body.

### 3. MODELLING

Mathematical modelling of the Karman vortex street seems to be the most powerful method leading to understand the phenomena. In the case of the vortex meter, the problem is extremely difficult, because of many factors influencing the phenomenon. So, its description is very complicated.

Navier-Stoke's equations describe the phenomena appearing in the vortex meter, but their analytical solution is not yet known. Attempts of a numerical solution of the N-S equations have not been successful for a long time because of lack of enough speed and memory of contemporary computers.

Other approaches - not based on Navier-Stoke's equations - have been performed in the meantime. Works presented in [24-28] have been based on potential flow around the bluff body. Discrete vortices generation has been modelled due to boundary layers and shear layers superposition.

Recent fast development of the computational technique has enabled considerable progress in numerical modelling of the vortex meter. In spite of the fact that some authors sometime even negated the feasibility of useful numerical modelling application in vortex meter design [2, 29], significant results have been attained in the last years. Especially valuable works have been carried out by researchers from the University of Essen. Due to investigations conducted in parallel, on a measuring stand and with CFD software - the reference to real phenomena has been attained. Designing of a new bluff body shape can be stated as the most spectacular result of the modelling [30].

### 4. MODEL IDEA

The proposed model is based on observation of the Karman vortex street phenomenon (results of the hot-wire anemometer investigations and flow visualisation). The most important remarks are:

- vortices originate alternatively on both sides of the bluff body and roll downstream,
- the diameter of each vortex increases with its displacement,
- traces of vortices cover a limited area,
- downstream the bluff body a „slow motion” area is distinguished,
- vortices take places subsequently with their alternative rotation respectively creating the Karman street,
- outside the Karman street area the flow is undisturbed.

The existence of the “low motion” area downstream the bluff body has been already suggested by Birkhoff [22] as a factor being conducive to vortex generation. Also laboratory investigations made by the authors of the article confirmed the existence of this area.

On the basis of above remarks the two-dimensional model of the Karman vortex street has been created. As shown in Fig. 2 the circular cylinder as the bluff body is appointed in the duct bound by the walls.

Eddies arise on the bluff body surface in the area of boundary layer separation. Then they grow-up rolling downstream on the surface of the stagnation region. Succeeding layers are added to the vortex, hence its diameter and energy grow-up.

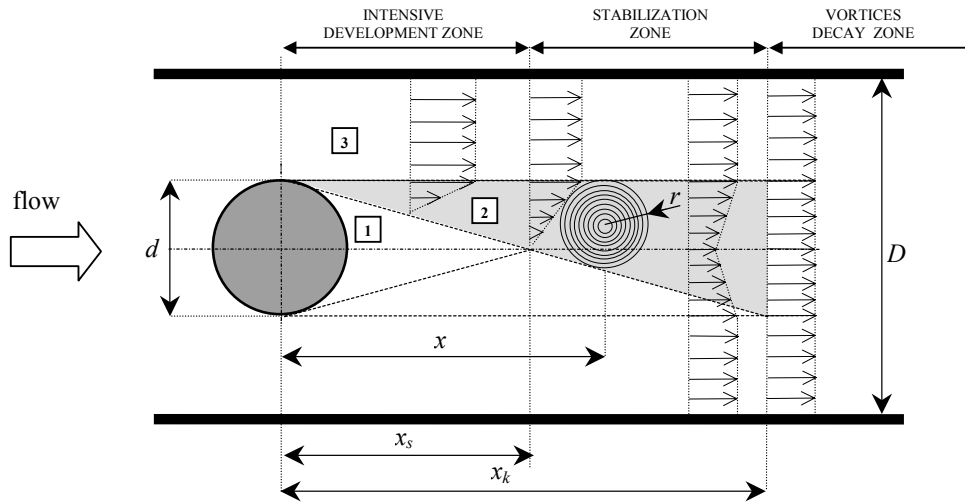


Fig.2. Development of consecutive vortices downstream the bluff body (1 - stagnation region, 2 - region of vortices development, 3 - region of steady velocity profile).

Regarding different vortex development phases, the area downstream the body has been divided into three zones:

- intensive development zone
- stabilization zone
- vortices decay zone.

In the **intensive development zone**, rapid growing-up of the vortices occurs. Three regions in the zone may be distinguished: stagnation region, region of steady velocity profile and region of vortices development.

The wedge-shaped **stagnation region** (**1** in Fig. 2) is located downstream the bluff body. The region may be treated as a rigid body on which both sides the vortices roll down alternatively. The diameter of the vortex increases along with its downstream movement. Inside the stagnation region no well-ordered fluid movement can be distinguished.

In the **region of steady velocity profile** (**3** in Fig. 2) there is no disturbance. The increase of local velocity is caused by damming up of the stream by the bluff body. To simplify the model it is assumed that the velocity vectors in this region are parallel. In fact, fluid from the region of steady velocity profile is taken to the region of vortices development.

In the **region of vortices development** (**2** in Fig. 2) the eddies, after originating on the bluff body surface, rapidly grow-up. The diameter of the vortex increases with its downstream movement. It is assumed that the vortex development is coaxial by an “adding layer” process satisfying the layer mass and geometry conservation principle. Each layer rotates respectively to local conditions at the moment of attachment. The number of layers increases with vortex displacement in time respecting the geometrical structure of the model. Each layer rotates with a constant origin rate until the viscous mechanism is applied.

In the **stabilization zone** a further, but considerably slower than previously, vortex development is performed. In this zone, only two regions may be distinguished: region of vortices development and region of steady velocity profile.

In the **intensive decay zone** vortices floated with the stream lose their energy and gradually fade.

#### 4.1. Model foundations

Because of varying vortex development conditions, the vortex development must be considered separately in each zone.

##### 4.1.1. Intensive development zone

Due to the bluff body location in the duct, the local damming up of the fluid, a local increase of the flow velocity is observed. Accordingly to the stream continuity principle, the equation is fulfilled:

$$vD = \int v_{px} dy . \quad (2)$$

Hence at the point of maximal fluid swelling:

$$v_{p0} = \left( \frac{D}{D-d} \right) v . \quad (3)$$

In the first approximation, the point of maximal swelling may be found as the point of vortex generation (boundary layer separation). It is not quite true, because the separation angle changes and in fact it may differ from 90°. It was also assumed that a wedge-shaped area of apparent unmoving fluid exists downstream the bluff body. The area will be further called the stagnation region. It is necessary to mention that the existence of the stagnation region, suggested already by Birkhoff [22], appears as an important factor in vortex development. It results in a variation of the velocity distribution downstream the bluff body. Obviously, the flow velocity is equal to zero on the stagnation region border. On the other hand, the flow velocity is uniform in the region of undisturbed flow. Hence we assume that the flow velocity varies linearly in the region of vortices development (at the moment of lack of vortex). Because of the existence of the wedge-shaped stagnation region, the stream velocity in the region of steady velocity profile decreases along with the distance  $x$  from the bluff body. It is necessary to underline that this is the velocity which is driving the created outer layer of the vortex. The velocity is expressed by the equation:

$$v_{px}(x) = v \frac{D}{D-d + \frac{d}{2} \cdot \frac{x}{x_s}} . \quad (4)$$

It is worth to notice that in the proposed model the velocity distribution inside the region of the intensive development zone does not influence the process.

#### **Vortex origin and development**

Vortices are created on the bluff body surface as the result of boundary layer separation. Then they grow-up increasing in their dimension and energy. The vortex dimension increase with its displacement from the point of the origin may be described within the model by the relationship:

$$r(x) = \frac{d}{4} \cdot \frac{x}{x_s} \quad (5)$$

In the intensive development zone the vortex rolls-up on the border between the stagnation region and the region of vortex development. On the other hand - the stream on the border of steady velocity profile forces the vortex.

In the model it was assumed that the vortex enlargement is related to the consecutive layers attachment. The rotation of every new vortex layer is caused by the stream velocity on the border of steady velocity region.

The rolling vortex motion may be treated as the sum of rotation and translation (Fig. 3).

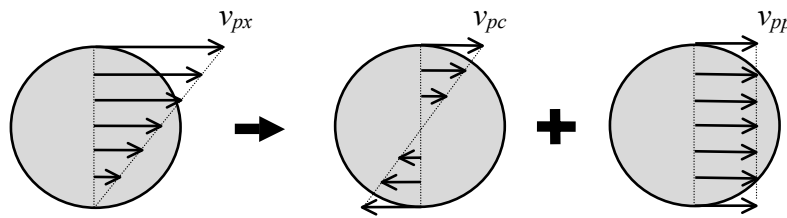


Fig.3. Vortex motion as the sum of rotation and translation in the intensive development zone.

Hence the velocity effectively forcing the layer rotation is given by:

$$v_{pc}(x) = \frac{v}{2} \cdot \frac{D}{D - d + \frac{d}{2} \cdot \frac{x}{x_s}} \quad (6)$$

As the result of above assumptions, the vortex translation velocity in the vortex development zone reaches the same value:

$$v_{pp}(x) = \frac{v}{2} \cdot \frac{D}{D - d + \frac{d}{2} \cdot \frac{x}{x_s}} \quad (7)$$

At the end of the vortex development zone the vortex diameter is equal to half of the bluff body diameter.

#### 4.1.2. Stabilization zone

Continued, but considerably slower vortex development in the stabilization zone was noticed. Although the geometrical enlargement of the vortex remains a linear function of its position, the vortex energy increases slower. In the stability zone the upper and lower verges of the vortex are forced by velocity vectors of the same direction, but of different values. The superposition formula may also be applied (Fig. 4).

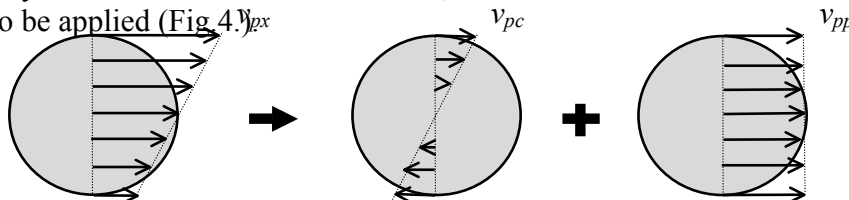


Fig.4. Vortex motion as the sum of rotation and translation in the stabilization zone.

Hence the velocity forcing the currently added layer rotation is expressed by equation:

$$v_{pc}(x) = \frac{v}{2} \cdot \frac{(2x_s - x)(x_k - x)}{(x_k - x_s)(1 - d/2D)x_s}. \quad (8)$$

The vortex translation velocity differs from  $v_{pc}$  and is expressed by equation:

$$v_{pp} = v \frac{D(x_k + x - 2x_s) - d(x - x_s)}{(2D - d)(x_k - x_s)}. \quad (9)$$

As results from Eq. (9), the translation velocity slightly increases along the distance  $x$  from the bluff body.

#### 4.1.3. Vortex decay zone

Although the vortex in sequel grows-up in the decay zone due to the viscosity forces, the rotation of added layers is equal zero. Hence any increase of vortex energy is not feasible in this zone. Because of the effect of viscosity forces inside the vortices, they loose their energy and gradually disappear.

### 4.2. Energy analysis

As it was mentioned earlier, the vortex energy grows with the vortex enlargement in the process of the attachment of new fluid layers accordingly to geometrical conditions. Each new layer is attached with its own velocity equal to the velocity of the fluid (called the “driving velocity”) assumed as constant for the whole new layer. The value of this velocity is the actual value on the border between the region of steady velocity profile and the region of vortice development. Hence the increase of vortex energy derives from the stream energy.

The angular velocity of the currently added layer (at the distance  $x$  from the axis of the bluff body) depends on  $v_{pc}$  as well as on the current vortex diameter:

$$\omega(x) = \frac{v_{pc}(x)}{2\pi r(x)}, \quad (10)$$

where  $r(x)$  is expressed by Eq. (5).

From a practical point of view, the most important parameter of the vortex is its rotation energy:

$$E_{rot} = \frac{1}{2} J \omega^2, \quad (11)$$

where the momentum of inertia for the circular cylinder - in 2D model (the vortex layer is the circular cylinder shape) - is expressed by:

$$J = m \frac{r^2}{2}. \quad (12)$$

In the model, the vortex consists of a certain number of coaxial layers, so the momentum of inertia for each layer might be calculated on the basis of equation:

$$J_k = \frac{1}{2} m_k (r_k^2 + r_{k-1}^2). \quad (13)$$

The mass of the layer is expressed by equation:

$$m_k = \pi (r_k^2 - r_{k-1}^2) \rho \Delta z. \quad (14)$$

The rotation energy of the  $k$ -th layer is expressed by:

$$E_{rot(k)} = \frac{1}{2} J_k \omega_k^2. \quad (15)$$

The rotation energy of the vortex has been calculated as the sum of energies for all layers:

$$E_{tot} = \sum_{k=1}^n E_{rot(k)}. \quad (16)$$

All considerations mentioned above were focused at the rotation energy as the parameter determining the magnitude of the measuring signal in the vortex meter.

### 4.3. Viscosity impact

Each layer of the vortex gets the rotation respectively to the point of its attachment. The difference between the adjacent layers rotation is the source of their viscous interaction. It is assumed that the momentum transfer proceeds simultaneously with the vortex enlargement process. The energy from higher rotation layers is transferred to lower rotation layers. The difference of rotation of the adjacent layers tends to zero with time.

Let us consider the viscous interaction between adjacent layers with different angular velocities  $\omega_k$  and  $\omega_{k-1}$ . The angular velocities resulting from the interaction process are:  $\omega_k'$  and  $\omega_{k-1}'$ .

The conservation of momentum principle has been applied. Absolute values of momentum transferred from each adjacent layers are equal, but of opposite signs:

$$J_k (\omega_k - \omega_k') = -J_{k-1} (\omega_{k-1} - \omega_{k-1}'). \quad (17)$$

The difference of angular velocities of the layers cause the momentum change. The related impulse of a force is expressed by equation:

$$P_0 = Fr\Delta t . \quad (18)$$

According to the dynamic viscosity factor definition:

$$\eta = \frac{F}{A} \cdot \frac{\Delta r}{\Delta v} \quad (19)$$

the interaction force between the adjacent layers may be calculated:

$$F = 2\pi r \Delta z \eta \frac{\Delta v}{\Delta r} . \quad (20)$$

Because:

$$\Delta v = \Delta \omega r \quad (21)$$

hence:

$$F = 2\pi r^2 \Delta z \eta \Delta \omega \frac{1}{\Delta r} , \quad (22)$$

$\Delta r$  means the thickness of the “interlayer” width where viscous interaction occurs. It was assumed that it has the value 0.5 of the outer layer and 0.5 of the inner layer width. As it was earlier assumed, all layers have a constant thickness:

$$\Delta r = \frac{r}{k} . \quad (23)$$

Finally:

$$P_0 = Fr\Delta t = 2\pi r^2 \Delta z \eta \Delta \omega k \Delta t . \quad (24)$$

Due to the fact that changes of momentum for both adjacent layers are equal but of opposite signs, a system of equations can be written:

$$\begin{cases} J_{k-1}(\omega_{k-1} - \omega'_{k-1}) = 2\pi r^2 \Delta z \eta \Delta \omega k \Delta t \\ -J_k(\omega_k - \omega'_k) = 2\pi r^2 \Delta z \eta \Delta \omega k \Delta t \end{cases} \quad (25)$$

taking into consideration the fact that the difference of angular velocity of both layers at the moment of the beginning of interaction is:

$$\Delta \omega = \omega_{k-1} - \omega_k . \quad (26)$$

Finally, angular velocities of both layers after their interaction during the time  $\Delta t$  are:

$$\begin{cases} \omega'_{k-1} = \omega_{k-1} - \frac{2}{J_{k-1}} \pi r^2 \Delta z \eta k \Delta t (\omega_{k-1} - \omega_k) \\ \omega'_k = \omega_k + \frac{2}{J_k} \pi r^2 \Delta z \eta k \Delta t (\omega_{k-1} - \omega_k) \end{cases} \quad (27)$$

It is necessary to remind that the process of energy exchange has a continuous character and its division into steps is done only for the calculation process. On the basis of determination of angular velocities of each layer, the rotation energy may be calculated. Hence calculation of the total rotation energy of the vortex is feasible.

## 5. CONCLUSIONS

The proposed model of the vortex development is based on the application of fundamental formulas. The vortex development has been divided into three stages. They differ from each other considerably and have been described by different equations. Due to application of the model, the fundamental parameters related to the vortex energy may be calculated. The viscosity impact on Karman vortex development has been also analysed. It has caused both: an energy exchange among the rotating layers as well as energy losses. Results of simulations of Karman vortex street development using the described model are presented in [31] - in the next issue.

## NOTATION

$f$	- vortex shedding frequency
$S_T$	- Strouhal number
$d$	- bluff body diameter
$v$	- flow velocity upstream the bluff body
$v_{pc}$	- flow velocity 'driving' the vortex
$v_{px}$	- current flow velocity at the distance $x$ from the pipe axis
$v_{p0}$	- flow velocity at the point of maximal fluid swelling
$v_{pp}$	- vortex translation velocity
$\omega$	- vortex angular velocity
$x$	- current vortex displacement from the bluff body axis
$x_s$	- length of intensive development zone
$x_k$	- length of intensive development and stabilization zones
$D$	- width of the pipe
$r$	- radius of the vortex
$\Delta z$	- width of the layer
$F$	- interaction force between the adjacent layers
$A$	- surface area between adjacent layers
$\rho$	- fluid density
$m$	- mass
$\eta$	- dynamic viscosity
$J$	- moment of inertia
$E_{rot}$	- rotation energy of the layer

- $E_{tot}$  - total rotation energy  
 $k$  - layer number

## REFERENCES

1. Cousins T., Foster S.A., Johnson P.A.: *A linear and accurate flowmeter using vortex shedding*. Proc. Power Fluid for Process Control Symposium, Inst. Measurement and Control, Guildford 1973, UK, pp. 45-46.
2. Cousins T.: *The performance and design of vortex meters*. Proc. Int Conf. Flow Measurement in the mid 1970's, Glasgow, UK.
3. Miller R.W., De Carlo J.P., Cullen J.T.: *A vortex flowmeter - calibration results and application experience*. Proc. Flow-Con 1977, Brighton, UK.
4. Kalkhof H.G.: *Influence of the bluff body shape on the measurement characteristics of vortex flowmeters*. Proc. of Conf. on Metering of Petroleum and its Products, 7-8 March 1985, London, UK.
5. Miao J.J., Wu C.W., Hu C.C., Chou J.H.: *A study on signal quality of a vortex flowmeter downstream of two elbows out-of-plane*. Flow Measurement and Instrumentation 13 (2002), pp. 75-85.
6. Lucas G.P., Turner J.T.: *Influence of cylinder geometry on the quality of its vortex shedding signal*. Proc. of International Conference on Flow Measurement FLOMEKO'85, 20-23 August 1985, Melbourne, Australia.
7. Bentley J.P.: *The development of a vortex flowmeter for gas flows in large ducts*. Proc. of International Conference on Flow Measurement FLOMEKO'85, 20-23 August 1985, Melbourne, Australia.
8. Pankanin G.L.: *A New Approach to the Bluff Body Design in Vortex Flowmeters*. Proc. of International Symposium on Fluid Control and Measurement FLUCOME TOKYO'85, Japan, pp. 1029-1034.
9. Pankanin G.L., Pytlak T.: *New Development in Vortex Meter Design*. Proc. of International Symposium on Fluid Control Measurement, Mechanics and Flow Visualisation FLUCOME'88, Sheffield, UK, pp. 479-483.
10. Igarashi T.: *Flow characteristics around a circular cylinder with a slit (1st report, Flow control and flow patterns)*. Bulletin of the JSME, no. 154, (1978), pp. 656-664.
11. Igarashi T.: *Flow characteristics around a circular cylinder with a slit (2nd report, Effect of boundary layer suction)*. Bulletin of the JSME, no. 154, (1978), pp. 1389-1397.
12. Popiel, C.O., Robinson D.I., Turner J.T.: *Vortex shedding from specially shaped cylinders*. Proc. of 11<sup>th</sup> Australasian Fluid Mechanics Conference, 14-18 December 1992, Australia, pp. 503-506.
13. Igarashi T.: *Fluid flow around a bluff body used for a Karman vortex flowmeter*. Proc. of International Symposium on Fluid Control and Measurement FLUCOME TOKYO'85, Japan, pp.1017-1022.
14. Pankanin G.L., Berliński J., Chmielewski R.: *Karman Vortex Street Visualization*. Proc. of International Symposium on Flow Visualization, Edinburgh 26-29 August 2000, UK, paper no. 239.
15. Pankanin G., Kulińczak A., Berliński J.: *Karman vortex street parametrization with image processing application*. Proc. of SPIE Optoelectronic and Electronic Sensors V, 2003, vol. 5124, pp. 186-192.
16. Pankanin G., Kulińczak A., Berliński J.: *Image Processing in Karman Vortex Street Identification*. Proc. of the 7<sup>th</sup> Triennial International Symp. on Fluid Control, Measurement and Visualization FLUCOME'03, Italy, 2003.
17. Pankanin G., Kulińczak A., Berliński J.: *Image Processing in Karman Vortex Street Identification*. Proc. of the 7<sup>th</sup> Triennial International Symp. on Fluid Control, Measurement and Visualization FLUCOME'03, Italy, 2003.
18. Terao Y., Choi H.M., Takamoto M., Matsui G.: *Measurement of Karman vortex street shed in a circular pipe using triple hot-wire probe*. Proc. of International Conference of Flow Measurement FLOMEKO'98, Sweden, pp. 197-201.
19. Terao Y., Choi H.M., Edra R. B., Takamoto: *An experimental study on flow structure in vortex flowmeters*. Proc. of International Conference of Flow Measurement FLOMEKO 1993, Korea, pp. 507-514.
20. Berliński J., Chmielewski R., Pankanin G.L.: *Vortex Flow Field Investigations with Application of Hot-Wire Anemometer*. Proc. of International Conference of Flow Measurement FLOMEKO 2000, Salvador, Brazil.
21. Pankanin G.L., Berliński J., Chmielewski R.: *Karman Vortex Street Visualization*. Proc. of International Symposium on Flow Visualization, UK, paper no. 239.
22. Birkhoff G.: *Formation vortex streets*. Journal of Applied Physics 24, no. 1 (1953), pp. 98-103.
23. Gerrard J.H.: *The mechanics of the formation region of vortices behind bluff bodies*. J. Fluid Mech. 25 (1966) pp. 401-413.
24. Chaplin J.R.: *Computer model of vortex shedding from a cylinder*, Journal of the Hydraulics Division, Proc. of the American Society of Civil Engineering, 1973, pp. 155-165.

25. Abernathy F.H., Kronauer R.E.: *The formation of vortex streets*. Journal of Fluid Mechanics, vol.13, part 1, 1962, pp.1-20.
26. Gerrard J.H.: *Numerical computation of the magnitude and frequency of the lift on a circular cylinder*. Philosophical Transactions, Royal Society of London, vol. 261, series A, 1967, pp. 137-162.
27. Sarpkaya T.: *An analytical study of separated flow about circular cylinders*. Journal of Basic Engineering, vol. 90, no.4, 1968, pp. 511-520.
28. Laird A.D.K.: *Eddy formation behind circular cylinders*. Journal of the Hydraulics Division ASCE, vol. 97, No. HY6, Proc. Paper 8170, June 1971, pp. 763-775.
29. Cousins T., Hayward A.J.T., Scott R.: *Design and performance of a new vortex shedding flow meter*. Proc. of IMEKO Dusseldorf 1989, pp. 151-163.
30. Hans V., Windorfer H.: *Comparison of pressure and ultrasound measurements in vortex flow-meters*. Measurement 33 (2003), pp. 121-133.
31. Pankanin G.L., Berlinski J., Chmielewski R.: *Simulation of Karman vortex street development using new model*, Metrology and Measurement Systems (in the next issue).

## ANALITYCZNE MODELOWANIE ŚCIEŻKI WIROWEJ

### Streszczenie

W artykule przedstawiono nowe podejście do problemu modelowania ścieżki wirowej Karmana. Wykorzystuje ono wnioski z obserwacji zjawiska i stanowi próbę opisanego prostymi zależnościami właściwymi dla fizyki klasycznej. Wiry powstają na powierzchni przeszkody w obszarze oderwania strugi. Proces wzrostu wiru polega na nawijaniu na jego rdzeń cienkiej warstwy płynu w miarę oddalania się od punktu oderwania. W modelu proces ten jest reprezentowany przez „obrastanie” wiru kolejnymi warstwami. Proces rozwoju został podzielony na trzy etapy. Zostały wyróżnione trzy strefy rozwoju wiru: intensywnego rozwoju, stabilizacji i zaniku. Przeanalizowano wpływ lepkości płynu na proces rozwoju i energię wiru.